Environment International 197 (2025) 109334

Contents lists available at ScienceDirect

Environment International

journal homepage: www.elsevier.com/locate/envint

Full length article

Genomic insights and metabolic pathways of an enriched bacterial community capable of degrading polyethylene

Qihao Li [a,1], Huixin Li [a,1], Li Tian [a], Yicheng Wang [a], Zeping Ouyang [a], Liguan Li [b], Yanping Mao [a,*]

[a] College of Chemistry and Environmental Engineering, Shenzhen University, Shenzhen, Guangdong 518071, China
[b] Department of Science and Environmental Studies, The Education University of Hong Kong, Hong Kong SAR, China

ARTICLE INFO

Handling Editor: Hefa Cheng

Keywords:
Plastic
Activated sludge
Polyethylene
Biodegradation
Metagenome

ABSTRACT

In the face of mounting global plastic pollution, especially concerning microplastics, biodegradation must be a sustainable solution. The key factor driving this technology is to explore efficient plastic-biodegraders from different habitats, among which activated sludge (AS) may be an important option since it holds diverse microorganisms occupying various ecological niches. Here we intend to enrich the plastic-degrading microorganisms from AS by using polyethylene (PE) plastic as the carbon and energy source. After a 28-day incubation, the weight loss of PE films reached 3% and the hydrophobicity decreased, indicating physical biodegradation. Moreover, Fourier-transform infrared spectroscopy (FTIR) results showed the formation of several new oxygen-containing functional groups on PE. Microbial analysis extracted 26 metagenome-assembled genomes (MAGs) from the enriched microbial communities. Among them MAG10, MAG21 and MAG26 displayed the increased abundance upon PE addition and harbored abundant genes related to carbohydrate transport and metabolism, suggesting their potential to degrade PE. Additionally, functional analysis revealed 14 plastic degradation-related genes, including oxidase, laccase, and lipase, indicating the significant potential in plastic degradation. Furthermore, a pathway for synergistic biodegradation of PE was proposed based on the potential PE degradation genes retrieved from MAGs. This work offers a promising and sustainable solution to plastic pollution by enriching the potential biodegraders from AS.

1. Introduction

As of 2023, global plastic production reached 413.8 million tons (Plastics Europe, 2024). Used plastic products are discarded at will, resulting in a large amount of plastic waste entering the environment, in which large plastic fragments are easily affected by physical, chemical and biological actions to decompose into small particles or fragments (Sun et al., 2020), and then form plastics with the diameter of less than 5 mm, also known as microplastics (MPs) (Thompson et al., 2004). MPs have the characteristic of a large specific surface area, which makes them easy to absorb pollutants (Tang et al., 2021), enrich pathogens (Junaid et al., 2022) and antibiotic resistance genes (Li et al., 2022). This poses a huge threat to human health and the ecological environment (Engler, 2012).

At present, the common disposal methods of plastic waste include landfill, incineration or chemical methods such as hydrolysis and oxidation to deconstruct plastics (Singh et al., 2022). Compared with common disposal methods, biological methods for degrading plastics have the characteristics of being economical and environmentally friendly. For example, strains that can efficiently degrade polyethylene terephthalate (PET) have been discovered, effectively converting PET into its two environmentally friendly monomers (Yoshida et al., 2016), and further using enzyme engineering to achieve complete hydrolysis of PET and the recycling of PET plastic monomers within a week (Lu et al., 2022). It can be seen that using microorganisms to degrade plastics has the advantages of green and efficient degradation, but its intrinsic enzymatic degradation mechanisms and microbial synergistic interactions have not yet been clearly revealed.

Polyethylene (PE) accounts for 26.2 % of global production and is one of the most widely used plastics (Plastics Europe, 2024). PE is a traditional fossil-based plastic, often used in plastic wrap, agricultural mulch and packaging materials. Its wide use causes serious pollution to

* Corresponding author.
E-mail address: maoy@szu.edu.cn (Y. Mao).
[1] These authors contributed equally to this work.

https://doi.org/10.1016/j.envint.2025.109334
Received 20 November 2024; Received in revised form 5 February 2025; Accepted 14 February 2025
Available online 15 February 2025

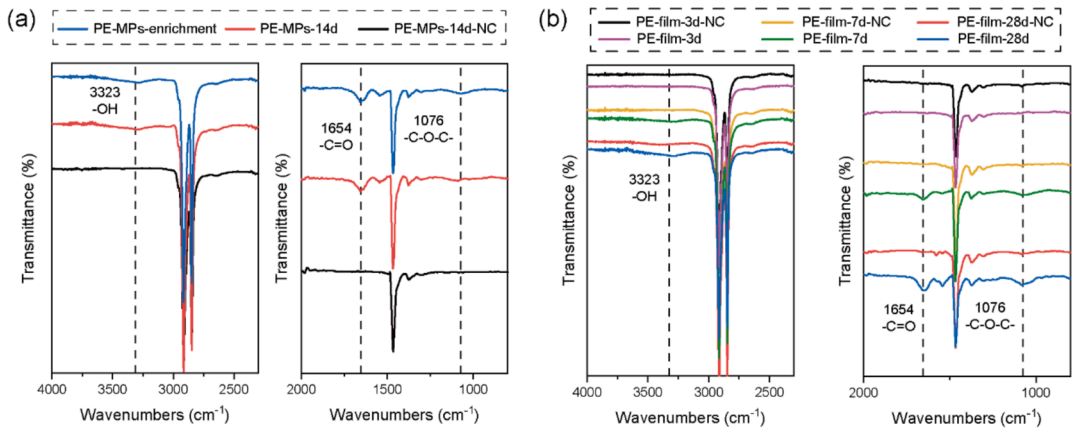

Fig. 1. Changes of functional groups on PE incubated with or without the AS microbial community. (a) FTIR spectra of PE MPs in enrichment culture after about 10 weeks (blue line) and FTIR spectra of PE MPs after 14 d of incubation with (red line) or without (black line) the enriched microbial community. (b) FTIR spectra of PE films during 28 d of incubation with (purple line, green line and blue line) or without (black line, yellow line and red line) the enriched microbial community. (For interpretation of the references to colour in this figure legend, the reader is referred to the web version of this article.)

the natural environment, making the management and mitigation of PE plastic waste urgent. Common sources of PE degraders include insects (Yang et al., 2014; Yang et al., 2015), soil (Kim et al., 2021; Kumar et al., 2024), activated sludge (AS) (Yue et al., 2021) and mangrove environment (Liu et al., 2023), among which AS has abundant resources, low economic cost and better biosecurity. In recent years, a variety of environmental bacteria have been found to be able to degrade plastics, especially PE plastics, but the biodegradation rate remains limited. According to research, *Stenotrophomonas pavanii* (Mehmood et al., 2016) caused a 3 % weight loss in the tested PE after 56 days, while *Alcanivorax* sp. (Zadjelovic et al., 2022) resulted in only 0.9 % weight loss after 34 days. Compared to a single strain, a microbial consortium of *Arthrobacter* sp. and *Streptomyces* sp. had a much greater impact on the degradation of PE films, demonstrating that the microbial community may enhance plastic degradation (Han et al., 2020). Notably, studies have found that AS communities have the ability to degrade persistent pollutants such as polychlorinated biphenyls and polycyclic aromatic hydrocarbons (Grandclément et al., 2017). More importantly, AS contained microorganisms associated with plastic degradation (Li et al., 2022). Therefore, utilizing AS communities for the synergistic degradation of polyethylene (PE) plastic holds great potential. However, current research on the degradation of PE by AS communities remains limited, it is unclear which microorganisms are involved in the synergistic degradation of PE and which enzymes regulate the PE degradation pathways, necessitating further investigation.

Therefore, in this study, we use a culture-based method to enrich the PE-degrading microbial communities from AS, evaluate its biodegradation characteristics, and reveal the potential degradation pathway, aiming to (1) clarify whether the selectively enriched microbial community has the potential for plastics biodegradation, (2) evaluate the plastic biodegradation ability of the microbial community, (3) elucidate potential biodegradation pathway of PE. This study highlights the possibility of efficient degradation of PE by the potential synergistic effect of the whole microbial community, and deepens our understanding towards the metabolic mechanism of PE biodegradation.

2. Materials and methods

2.1. Pretreatment of PE plastics

Two types of PE plastics were used in this study, one was PE microplastics with a size of 16 mesh (particle size about 1.18 mm), which was purchased from Dongguan Huachuang Plastic Chemical Co., Ltd. (Guangdong, China), and another was the PE film purchased from Guangzhou Zhichuang Packaging Materials Co., Ltd. (Guangdong, China), with a thickness of 0.020 mm, the film was cut into 30 mm × 30 mm thin slices for experiments. In order to remove impurities on the surface of PE as much as possible, all plastics were soaked in 75 % ethanol for 15 min and rinsed with ultrapure water 3 times, and air-dried on an ultra-clean bench (Zhang et al., 2022b).

2.2. Culture enrichment for PE degradation

AS samples were collected from an aeration tank of NS municipal wastewater treatment plant (113.91°E, 22.52°N) in Shenzhen, Guangdong Province, China. Subsequently, 6 mL AS and 0.2 g PE MPs were added into 100 mL mineral salt medium (MSM) and incubated in a shaking incubator at 30 °C, 150 rpm for enrichment. Every two weeks, Fourier-transform infrared spectroscopy (FTIR) analysis was performed on PE MPs to assess whether PE MPs had been degraded. The mineral salt medium was composed of 0.6 g/L NaCl, 0.7 g/L NH_4Cl, 0.32 g/L K_2HPO_4, 0.4 g/L NaH_2PO_4, 0.25 g/L $MgSO_4$, 0.1 g/L $CaCl_2$, 0.05 % w/v yeast extract and 0.2 % trace element solution (TES). The constituents of TES are presented in the supporting information (SI) Table S1.

2.3. PE degradation by the enriched community

PE MPs and PE films were added separately for PE degradation experiments to verify the degradability of the enriched microbial community from AS. Since oxygen-containing functional groups were formed on PE MPs in the enrichment culture at about 10 weeks (Fig. 1a), suggesting the biodegradation of PE, we chose the enrichment culture after about 10 weeks of incubation as the inoculum for the PE degradation experiment. For PE MPs, the experimental group was added PE MPs (0.2 % w/v) and inoculated with the enriched culture (6 % v/v), the positive control (PC) group was only incubated with enrichment culture but not added PE MPs, and the negative control (NC) group was only added PE MPs but not incubated with the enriched community. The experimental group, the PC group and the NC group were all cultivated in triplicate. All cultures were incubated in 100 mL Erlenmeyer flask with 40 mL MSM using the shaking incubator at 30 °C, 150 rpm for 14 d without replacing the culture media.

The incubation conditions and group settings of the PE films were consistent with the experimental design of PE MPs (i.e. experimental group, PC group and NC group). But for the experimental group and the NC group, the incubation time was set to 3 d, 7 d, and 28 d, respectively to observe and compare to the degrading effects of PE films. Since the PC group was not added with PE films, the culture medium lacked a continuous carbon source, resulting in a significant reduction in microbial biomass and loss of microbial activity at 7 d. (Fig. S2b), so the

microbial community was only incubated for 3 d and 7 d in PC group. The OD_{600} values of experimental and PC groups were measured to characterize the microbial growth, and each group was measured in triplicate.

2.4. Characterization of PE plastics

After the incubation, all PE MPs and PE films were retrieved and the biofilm on PE surface was cleaned as thoroughly as possible before biodegradation characterization according to the procedure of the previous study (Zhang et al., 2022b). The films were firstly soaked in 2 % (w/v) sodium dodecyl sulfate (SDS) aqueous solution and shaken for 4 h at 100 rpm. And then, the PE was transferred into a new 2 % (w/v) SDS aqueous solution and soaked at 50 °C for 12 h. Finally, the PE was rinsed with sterile water and dried in a laboratory oven at 50 °C until constant weight. The cleaned PE films were used to characterize the biodegradation effect by weight loss, contact angle and FTIR analysis. Due to the small particle size of PE MPs, it was difficult to perform weight loss and contact angle testing, so only FTIR analysis was performed on this material. The PE films before and after incubation were weighed (n = 3) using a 4-decimal place electronic balance, and the percentage weight loss of the films was calculated according to the following equation. M_I and M_F represent the initial films weight before incubation and the final films weight after incubation, respectively.

$$Percentage\ weight\ loss = (M_I - M_F) / M_I \times 100\%$$

The changes in hydrophilicity on the surface of PE films were detected by contact angle analysis using a water contact angle measuring device (SDC-350, Dongguan Dingsheng Precision Instrument Co., Ltd., China). The drop volume of deionized water was set to 5 μL. An attenuated total refraction FTIR spectrometer (IR Affinity-1, Shimadzu, Japan) was used to analyze the changes of PE surface functional groups and surface chemical components. The spectra were taken from 4000 to 500 cm^{-1} with a spectral resolution of 4 cm^{-1} over 30 scans. Absorbance and transmittance were recorded and the FTIR spectra were further smoothed, baseline normalized, and plotted using Origin Pro 2021 (Peng et al., 2022).

2.5. Metabolite analysis

The metabolite composition of the experimental group and PC group was detected by high performance liquid chromatography-tandem mass spectrometry (HPLC-MS/MS). After the incubation of 7 d, cultures containing the microbial community with or without PE films were collected and filtered by sterile PTFE membranes (pore size 0.45 μm). One mL filtrates were then freeze-dried and centrifuged at 15,000 × g for 15 min at 4°C after adding 100 μL 80 % aqueous solution of methanol. The supernatants were diluted to a final concentration containing 53 % methanol by liquid chromatography-mass spectrometry (LC-MS) grade water. The diluted samples were subsequently centrifuged again at 15,000 × g for 15 min at 4°C, and the final supernatants were collected for HPLC-MS/MS analysis. HPLC-MS/MS analysis was performed on a Vanquish UHPLC system (Thermo Fisher, Germany) equipped with an Orbitrap Q Exactive ™ HF-X mass spectrometer (Thermo Fisher, Germany). Samples were injected into a Hypesil Gold column (100 × 2.1 mm, 1.9 μm) at a flow rate of 0.2 mL/min and a column temperature of 30 °C. The eluents for the positive polarity mode were 0.1 % formic acid in water (eluent A) and methanol (eluent B). The eluents for the negative polarity mode were 5 mM ammonium acetate (eluent A) and methanol (eluent B). The elution condition was set as follows: 2 % B, 1.5 min; 2–85 % B, 3 min; 85–100 % B, 10 min; 100–2 % B, 10.1 min; 2 % B, 12 min. The identified metabolites were annotated by KEGG, HMDB and LIPIDMaps databases. Principal components analysis (PCoA) and orthogonal partial least squares discriminant analysis (OPLS-DA) were used to differentiate the metabolite profiles between the experimental group and PC group. PERMANOVA test (999 permutations) based on the Bray-Curtis distance was used to determine the significant differences in metabolites between the experimental group and PC group. *P* values were calculated using t tests and then adjusted by Benjamini-Hochberg's approach. The identified metabolites with thresholds of adjusted *P* value < 0.05 and fold change ≥ 1.2 were considered as significantly different metabolites. Volcano plot was illustrated to identify the differential metabolites between the experimental and PC groups.

2.6. DNA extraction, metagenomic sequencing and analysis

After 7 d of incubation, 30 mL culture mixture solutions of the free-living community and PE-attached biofilm mixture from the experimental group, and 30 mL culture solutions from PC group were collected. Subsequently, the solutions were filtered using a vacuum filter pump with sterile PTFE membranes (pore size 0.45 μm). Total DNA was extracted from the membranes which filtered the culture solutions using the FastDNA® SPIN Kit for Soil (MP Biomedicals, USA) according to the manufacturer's protocol. Agarose gel electrophoresis was used to assess the DNA quality and NanoDrop (Thermo Fisher Scientific, USA) was used to measure the DNA concentration. Extracted DNA samples were stored in a −80 °C refrigerator until metagenomic sequencing.

Metagenomic sequencing was outsourced to Novogene Co., Ltd. (Beijing, China) to construct the libraries with an insert size of 350 bp, which was then sequenced on the Illumina NovaSeq 6000 platform using PE150 (paired-ended 2 × 150 bp) strategy to obtain the raw data for sequencing and quality control (QC). The QC process was based on Yan et al. (Yan et al., 2013), which removed non-biological adapter sequences and low-quality reads (Phred score Q20 ≤ 20) in the metagenomic data to ensure data quality. Finally, six samples (three samples from the experimental group and another three from the PC group collected after 7 d) generated approximately 81.1 GB clean metagenomic sequencing reads. The metagenomic sequencing data have been deposited in the Sequence Read Archive (SRA) of National Center for Biotechnology Information (NCBI) under the BioProject ID PRJNA1167014.

The clean reads from the same experimental group were co-assembled using MetaSPAdes v.3.13.0 (Bankevich et al., 2012). After assembly, contigs longer than 1000 bp were binned with metaBAT2 v.2.12.1 (Kang et al., 2019), MaxBin2 v.2.2.6 (Wu et al., 2016) and CONCOCT v.1.0.0 (Alneberg et al., 2014) using MetaWRAP v.1.3.2 pipeline (Uritskiy et al., 2018). CheckM v.1.0.12 with lineage-specific marker sets was used to assess the completeness and contamination of binned metagenomic assembled genomes (MAGs) (Parks et al., 2015). The MAGs were then refined using the refinement module in MetaWRAP, and only MAGs with quality score (completeness − 5 × contamination) ≥ 50 were retained (Saheb Kashaf et al., 2021). The resulting MAGs were dereplicated using dRep v.3.4.0 (Olm et al., 2017) with an average nucleotide identity (ANI) > 95 % because bacterial species boundaries are generally located at 95 % ANI. The dereplicated MAGs were aligned against Genome Taxonomy Database (GTDB) (Parks et al., 2020) for taxonomic annotation using GTDB-Tk v.2.1.0 based on 120 single-copy genes of bacteria (Chaumeil et al., 2020). Relative abundance of MAGs was calculated referring to the previous study (Reji et al., 2022). Abundances are expressed as the number of reads mapped per kilobase of genome per gigabase of metagenome (RPKG). The clean reads per sample were mapped against each MAG using Salmon v.1.9.0 (Patro et al., 2017). The relative abundance of MAGs was equal to the mapped reads divided by the product of the MAGs size (kilobase, Kb) and the metagenome size (gigabase, Gb). Phylogenetic trees were inferred under the model WAG + GAMMA using FastTree v.2.1.11 (Price et al., 2009) and the trees were visualized in the R package "ggtree" (Yu et al., 2017). Prodigal v.2.6.3 (Jin et al., 2023) was used to predict open reading frames (ORFs), and then the ORFs were functionally annotated with CAZy, COG, and KEGG databases (e value ≤ 1×10^{-5}) using

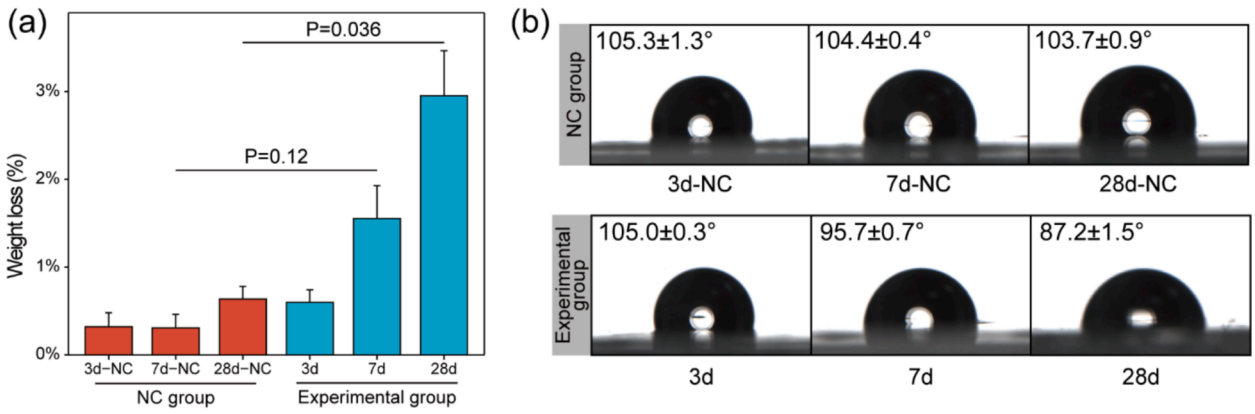

Fig. 2. Physical property changes of PE films during 28 d of incubation. (a) Weight loss of PE films with (experimental group) and without (NC group) the enriched microbial community. P-values (Student's *t*-test) showed the statistical difference between the weight loss of experimental group and NC group. (b) Contact angles of PE films with (experimental group) and without (NC group) the enriched microbial community.

eggNOG-mapper v.2.1.9 (Cantalapiedra et al., 2021).

3. Results and discussion

3.1. Changes in the functional groups and physical properties of PE produced by the selected enriched community

The AS community is a highly active biological community with a large number of microorganisms (Zhang and Zhang, 2023). To explore the degradation potential of AS community on PE, we inoculated AS into the medium with PE MPs to enrich PE-degrading microbiota. We checked the FTIR spectra of the PE MPs in the enriched culture every two weeks to assess whether PE MPs were being biodegraded. At about 10 weeks, we observed the formation of obvious oxygen-containing functional groups on PE (Fig. 1a), suggesting the biodegradation of PE. Therefore, we used the enriched microbial community after about 10 weeks of incubation as the inoculum for PE degradation experiments. The enriched microbial community could stably colonize on the PE films after 4 d (SI Fig. S1). Then the microbial community was used to perform the PE degradation experiments. The growth curves indicated that the microbial community in both experimental group and PC group showed a similar trend, the growth curve first increased and then decreased (SI Fig. S2). However, compared with those in the PC group, the growth of the community in the experimental group was higher, which suggested that PE could act as a carbon source for the enriched microbial community though the bioavailability of PE was not sufficient for the

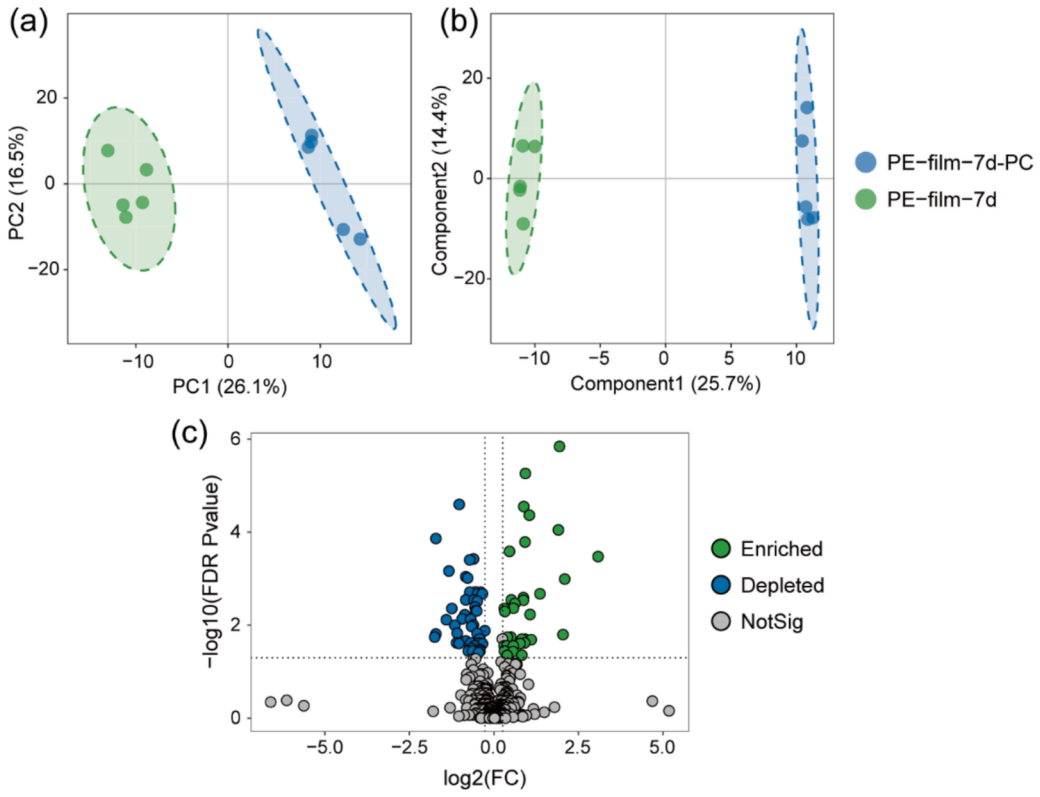

Fig. 3. Differences of metabolic characteristics between the experimental group (PE films added) and PC group (no PE films) after 7 d of incubation analyzed by HPLC-MS/MS. (a) The PCA plot of metabolites in experimental and PC groups. (b) The OPLS-DA plot of metabolites in experimental and PC groups. (c) The volcano plot of differential metabolites enriched and depleted in experimental compared with PC groups.

enriched community to maintain a high growth rate (Zadjelovic et al., 2022). Next, the FTIR analyses were performed to detect the changes of functional groups on PE after the incubation by the enriched microbial community. Compared with the NC group, the FTIR spectra of PE in the experimental group showed three extra peaks (Fig. 1), indicating the formations of ether bonds (−C-O-C-, ~1076 cm^{-1}), carbonyl groups (C=O, ~1654 cm^{-1}), and hydroxyl groups (–OH, ~3323 cm^{-1}). Especially, with the increase of cultivation time, the intensities of these three peaks on the surface of the PE films increased (Fig. 1b). The appearance of these absorption peaks indicated the formation of active functional groups and the oxidation on the PE surface by the enriched microbial community, which destroyed the stable and inert structure of PE and further provided reaction sites for downstream microbial assimilation and PE biodegradation (Yeom et al., 2022; Zhang et al., 2022a).

Furthermore, weight loss measurement and contact angle analysis were used to determine the changes in the physical properties of PE films. Fig. 2a represented the weight loss over time of the PE films in the experimental group and NC group. During the 28 d, the weight loss of the PE films incubated with the enriched microbial community increased consistently, while that of the NC group remained stable. After 28 d of incubation, the weight of PE films incubated with enriched microbial community decreased by 2.95 ± 0.73 %, which was significantly higher than that of NC group ($P = 0.036$). Therefore, the evidence of weight loss revealed the bioavailability of PE as a carbon source for microbiota. However, since PE as a type of nonhydrolyzable plastic is polymerized by C–C strong covalent bonds, enzymatic chain scission of PE is more challenging compared with hydrolysable plastics (Wright et al., 2020), resulting in the initial microbial depolymerization and degradation process of PE to be relatively slow (Miri et al., 2022).

The contact angles of the PE films in the experimental group were significantly changed compared with the NC group ($P < 0.001$, t test) (Fig. 2b), indicating that the enriched microbial community could effectively reduce the hydrophobicity of PE films. After 7 d, the contact angles of PE films inoculated with enriched microbial community decreased to 95.7 ± 0.7°, and after 28 d, the contact angles of the PE films further decreased to 87.2 ± 1.5°. Particularly, with the contact angle and hydrophobicity of PE films decreased, microbiota will be more likely to adhere and colonize on PE films, reducing PE resistance to microbial degradation (Wu et al., 2023; Yang et al., 2014).

Overall, the changes in the functional groups and physical properties of PE after inoculation indicated the biodegradability of PE by the enriched microbial community. For nonhydrolyzable plastics such as PE, the surface oxidation and oxygen incorporation process are initial depolymerization and degradation process (Ghatge et al., 2020; Wright et al., 2020). The appearance of oxygen-containing functional groups such as carbonyl, carboxyl and hydroxyl provides evidence for the bio-oxidation of PE and the oxidation of PE by microorganisms promotes the scission of PE carbon chains and the depolymerization of PE, which eventually lead to the biodegradation of PE (Zhang et al., 2022a).

3.2. Analysis of PE degradation metabolites by HPLC

To further detect the differences of metabolite composition between the experimental group and PC group after 7 d of incubation, HPLC-MS/MS analysis was performed. Total 506 metabolites were detected and quantified in the experimental group and PC group, mainly in the classifications of lipids and lipid-like molecules (65), organic heterocyclic compounds (58), and organic acids and derivatives (50). Both the PCA and OPLS-DA plots showed that experimental group and PC group were clustered separately (Fig. 3a, b), and the differences in metabolite profiles between experimental group and PC group were significant ($P < 0.001$, PERMANOVA test). Furthermore, the volcano plot was constructed to illustrate significantly differential metabolites between the experimental group and PC group after 7 d of incubation (Fig. 3c). Total 78 metabolites were considered as significantly differential metabolites, and among them, 33 metabolites were enriched and 45 metabolites were depleted in the experimental group (Fig. 3c). More metabolites classified as lipids and lipid-like molecules, organic heterocyclic compounds, and benzenoids were depleted, and more metabolites classified as organic oxygen compounds and alkaloids and derivatives were enriched (Table 1). Although we attempted to further identify potential degradation products of PE from various metabolites, identifying them remains challenging. Compared to plastics such as polyethylene terephthalate (PET) and polystyrene (PS), whose degradation products are easier to identify due to the presence of benzene (Qiu et al., 2024; Yoshida et al., 2016), the monomer of PE is alkane, which has no characteristic molecules, and it is difficult to distinguish from the metabolome which are potential PE degradation products or cellular secretions (Gao et al., 2022; Gao and Sun, 2021). However, the addition of PE caused significant changes of the metabolites' composition, showing evidence that PE can act as a carbon source for the microbiota, strongly suggesting that the PE was biodegraded into new chemical substances, which resulted in significant differences of metabolite profiles between the experimental group and PC group.

Table 1
Classification and enrichment/depletion information of significantly different metabolites.

SuperClass	Enrichment	Depletion
Unclassified	18	22
Organoheterocyclic compounds	4	5
Lipids and lipid-like molecules	4	11
Organic acids and derivatives	2	2
Organic oxygen compounds	2	0
Nucleosides, nucleotides, and analogues	1	1
Alkaloids and derivatives	1	0
Benzenoids	1	4

3.3. Retrieved MAGs from the enriched microbial community

To further explore the microbial community composition and MAGs profile of the enriched microbial community, DNA samples were extracted from the experimental group and PC group after 7 d of incubation for metagenomic sequencing and binning. 52 high-quality MAGs with completeness > 50 % and contamination < 5 % were recovered, and then were dereplicated using dRep. Finally, 26 MAGs were retained and the statistical information of 26 dereplicated MAGs is presented in SI Table S2. The completeness from all 26 dereplicated MAGs was higher than 75 %, and the contamination was less than 4 %. Interestingly, only 6 of the 26 MAGs from the enriched microbial community were annotated to the known species against GTDB with ANI > 95 %. Although 14 MAGs were annotated by certain species against GTDB, their ANI compared with closest placement species < 95 %, indicating that these 14 MAGs could be novel species. In addition, 6 of the 26 MAGs could not be matched to certain species from GTDB.

In order to further explore the composition of MAGs, the abundances of MAGs in the experimental group and PC group were calculated. Mapping percentages of reads to contigs and MAGs were 47.74 % ± 0.31 % and 42.86 % ± 1.75 % respectively (SI Table S3), showing the moderate read recruitment. As shown in Fig. 4a, MAG22 (Burkholderiaceae *Candidimonas*) was the MAG with the highest abundance (145.59 ± 40.79 RPKG) in the PC group, followed by MAG8 (Weeksellaceae *Chryseobacterium*), MAG4 (Micropepsaceae *Rhizomicrobium*), and MAG17 (Chitinophagaceae *Flavipsychrobacter*). However, in the experimental group, MAG10 (Spirosomaceae *Arsenicibacter*) became the dominant MAG (123.93 ± 50.85 RPKG), followed by MAG22 (Burkholderiaceae *Candidimonas*), MAG26 (Rhodanobacteraceae 66–474), MAG4 and MAG21 (Haliangiaceae JABFXX01). In addition, the abundances of MAG10, MAG21 and MAG26 in the experimental group were noticeably higher compared with PC group (MAG10: 3.14 times; MAG21: 6.33 times; MAG26: 12.34 times), from which it could be

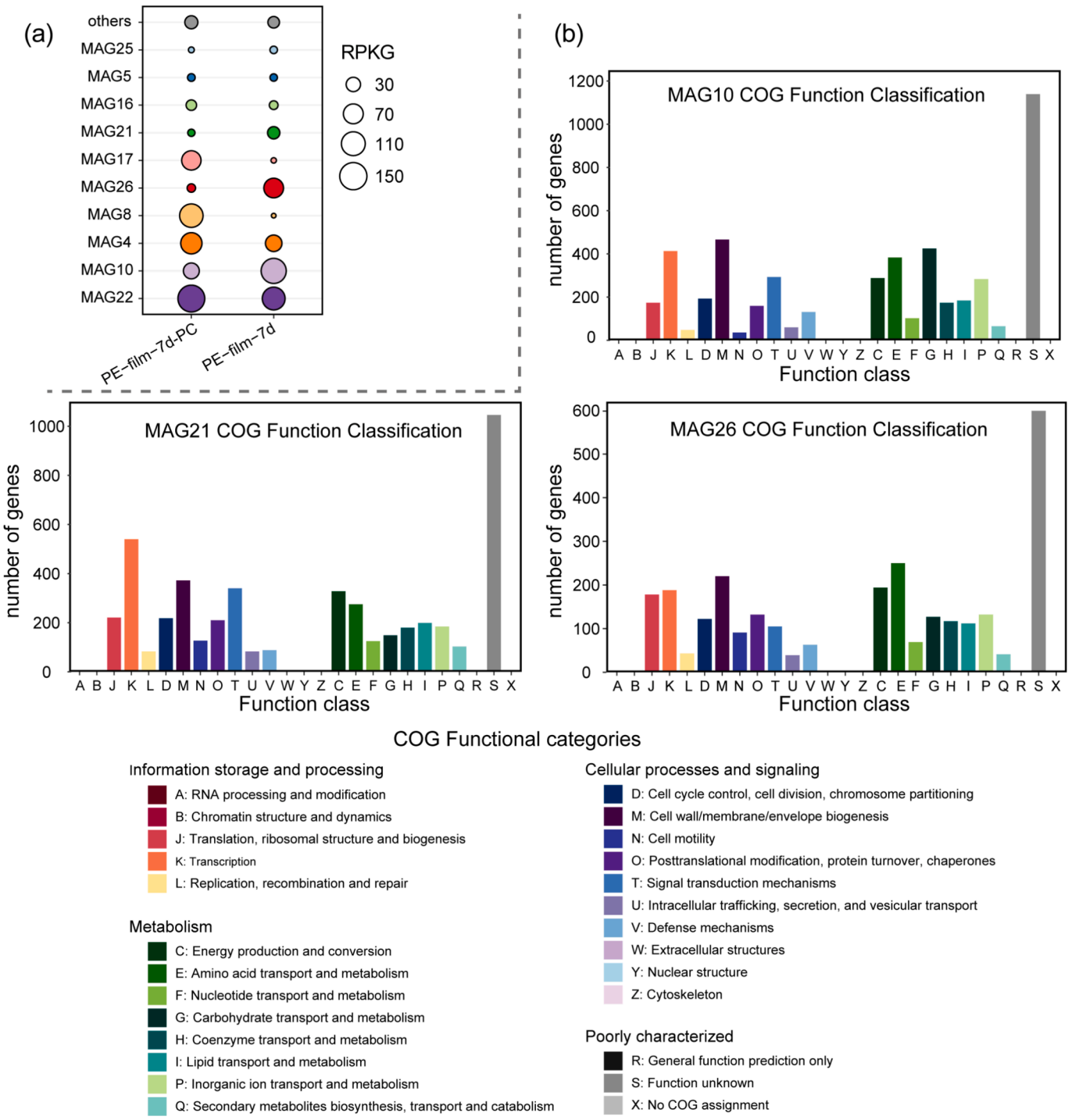

Fig. 4. (a) Abundance of the MAGs binning from the microbial community in experimental group and PC group after 7 d of incubation (reads mapped per kilobase of genome per gigabase of metagenome, RPKG). (b) Number of genes assigned to COG functional categories in MAG10, MAG21 and MAG26.

inferred that they played important roles in the process of degrading PE. Furthermore, these three MAGs contained abundant genes in the pathway of carbohydrate transport and metabolism, amino transport and metabolism, lipid transport and metabolism, etc. (Fig. 4b), and especially for MAG10 with multiple genes (425) in carbohydrate transport and metabolism which showed the potential to hydrolyze complex carbohydrates (Shen et al., 2022). However, which genes in the microbial community involved in which step of PE degradation remains unknown. Therefore, the gene annotations for 26 MAGs were further performed as follows to reveal the relevant functional genes involved in the PE degradation.

3.4. Potential PE degradation genes across the MAGs

To further reveal the relevant PE degradation genes in MAGs, gene prediction and annotation were performed, and a phylogenetic tree of MAGs was constructed based on single-copy marker genes. As shown in Fig. 5, multiple potential PE depolymerase genes were identified in MAGs from the enriched microbial community after 7 d of incubation. 23 of the 26 MAGs encoded laccase (Fig. 5), and as an important member of the multi-copper oxidase family, laccase plays an important role in the initial polymer oxidation and depolymerization of PE (Gao et al., 2022; Santo et al., 2013; Yao et al., 2022). In addition to laccase, 5 MAGs

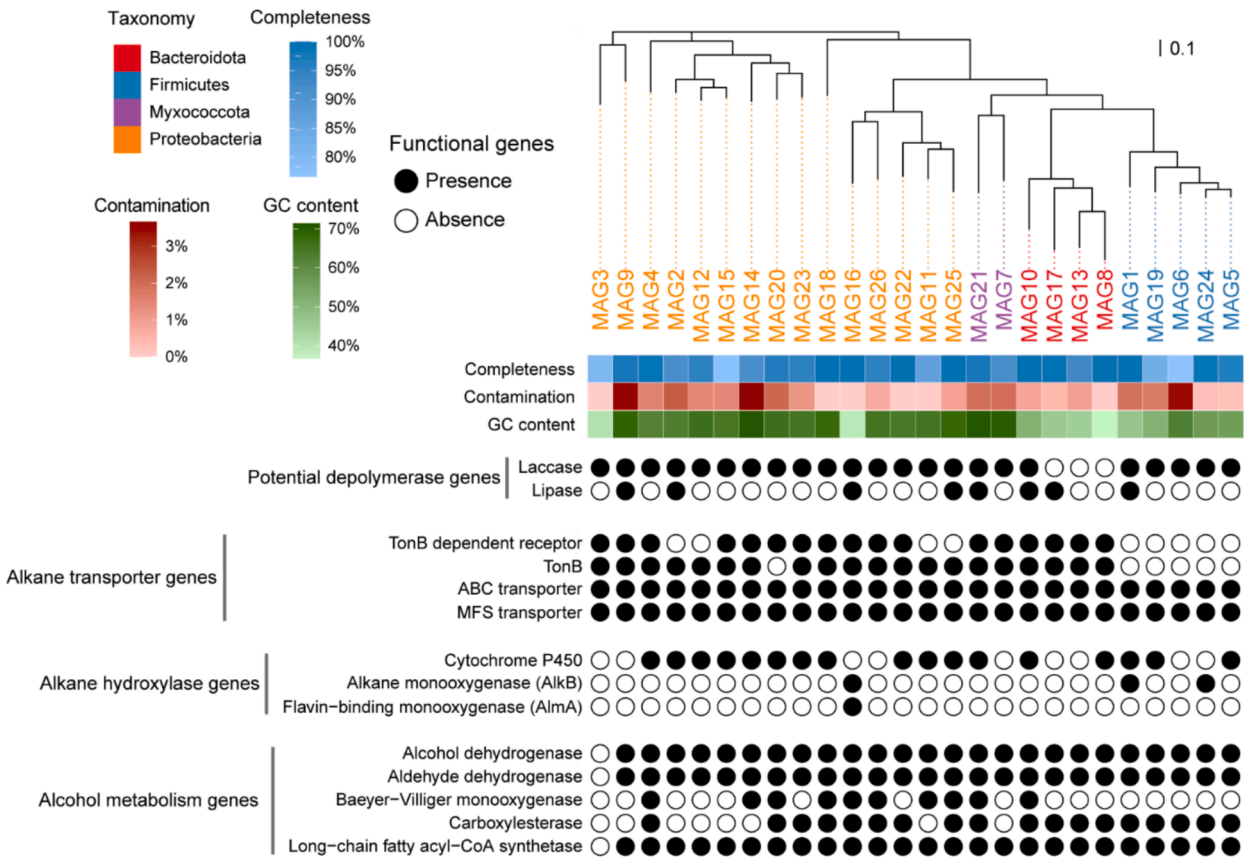

Fig. 5. Potential PE degradation genes across MAG phylogenetic clusters from the enriched microbial community after 7 d of incubation. The phylogenetic tree on the top was constructed using FastTree based on the maximum-likelihood method, with a concatenated set of single-copy marker genes. The colors of MAG ID indicate the phylum-level taxonomy of MAGs classified by GTDB. The heatmap indicated completeness, GC content, and contamination of the MAGs. The black solid circles represent the presence of the genes in MAGs, the white solid circles represent the absence of the genes in MAGs.

among the 26 MAGs also encoded lipase genes (Fig. 5), which could participate in the depolymerization of PE (Zadjelovic et al., 2022) and further hydrolyzed and converted the oxidized PE chains to oligomers or monomers. Several peroxidases, such as lignin peroxidase and manganese peroxidase (Santacruz-Juárez et al., 2021; Zhang et al., 2022a), have also been proposed to depolymerize PE, but these peroxidases were not found in the MAGs in this study.

When PE was depolymerized into monomer and small chain molecules (alkanes), the lower molecular weight allowed them to pass through the bacterial outer and inner membrane into the cytoplasm. Several membrane transporters, such as TonB-dependent outer membrane receptors, FadL and specific porins, were significantly highly expressed during the growth of the bacterium *Thalassolituus oleivorans* MIL-1 using long-chain alkanes (C28) as a carbon source (Gregson et al., 2018). In present study, multiple MAGs from Bacteroidota, Proteobacteria, and Myxococcota encoded TonB-dependent outer membrane receptors and TonB (Fig. 5). Accordingly, with the energy provided by TonB system (Postle and Larsen, 2007), TonB-dependent outer membrane receptors may transport alkanes from extracellular space to the periplasm by the active transportation. Interestingly, no MAGs from Firmicutes encoded TonB and TonB-dependent outer membrane receptor genes (Fig. 5), indicating a selective phylogenetic distribution of the TonB system among MAGs from the enriched microbial community. In addition, ATP-binding cassette (ABC) type and major facilitator superfamily (MFS) transporter as an inner membrane transporter can be significantly upregulated at the transcriptome and proteome levels during the bacterial growth on PE (Gravouil et al., 2017; Zadjelovic et al., 2022), which implied that the genes could transport alkanes into the cytoplasm. Therefore, all of 26 MAGs carry ABC and MFS transporter genes (Fig. 5), indicating the significant potential of the enriched microbial community in intaking and incorporating the PE oligomers or monomers (alkanes).

Hydroxylases, such as cytochrome P450 (Yeom et al., 2022), alkane monooxygenase (AlkB), and long-chain alkane monooxygenases (such as AlmA and LadA, etc.) (Rojo, 2009) can further oxidize alkanes into alcohols. Among the 26 MAGs, 3 MAGs encoded the AlkB, and for another hydroxylase, cytochrome P450, there were 17 MAGs encoding the gene of this enzyme (Fig. 5), indicating that the hydroxylation of alkanes by the enriched microbial community was mediated by both cytochrome P450 enzymes and AlkB. After hydroxylation, primary alcohols and secondary alcohols were generated, and subsequently alcohol dehydrogenase (Adh) in cytoplasm could further oxidize these alcohols to aldehydes and ketones respectively. For the aldehydes, aldehyde dehydrogenase (Aldh) can oxidize them to generate the long-chain fatty acids. Under the catalysis of long-chain acyl-CoA synthetase (ACSL), long-chain fatty acids can be transferred to acyl-CoA, enter the β-oxidation cycle, and are eventually metabolized and degraded by microorganism (Mashek et al., 2007).

The generated ketones can be further oxidized by another enzyme, Baeyer-Villiger monooxygenase (BVMO), which can insert an oxygen atom near the carbonyl carbon to create an ester (Yeom et al., 2022). The ester was easily hydrolyzed and cleaved by carboxylesterase to generate primary alcohols and long-chain fatty acids. The oxidation of primary alcohols was consistent with the above process. Eventually, one ester could generate two acids and enter the β-oxidation cycle and TCA cycle. It is worth noting that multiple MAGs (MAG4, MAG10, MAG16, MAG18, MAG20, MAG21 and MAG25) of the AS enriched community contained all genes in the alkane oxidation metabolic process, which

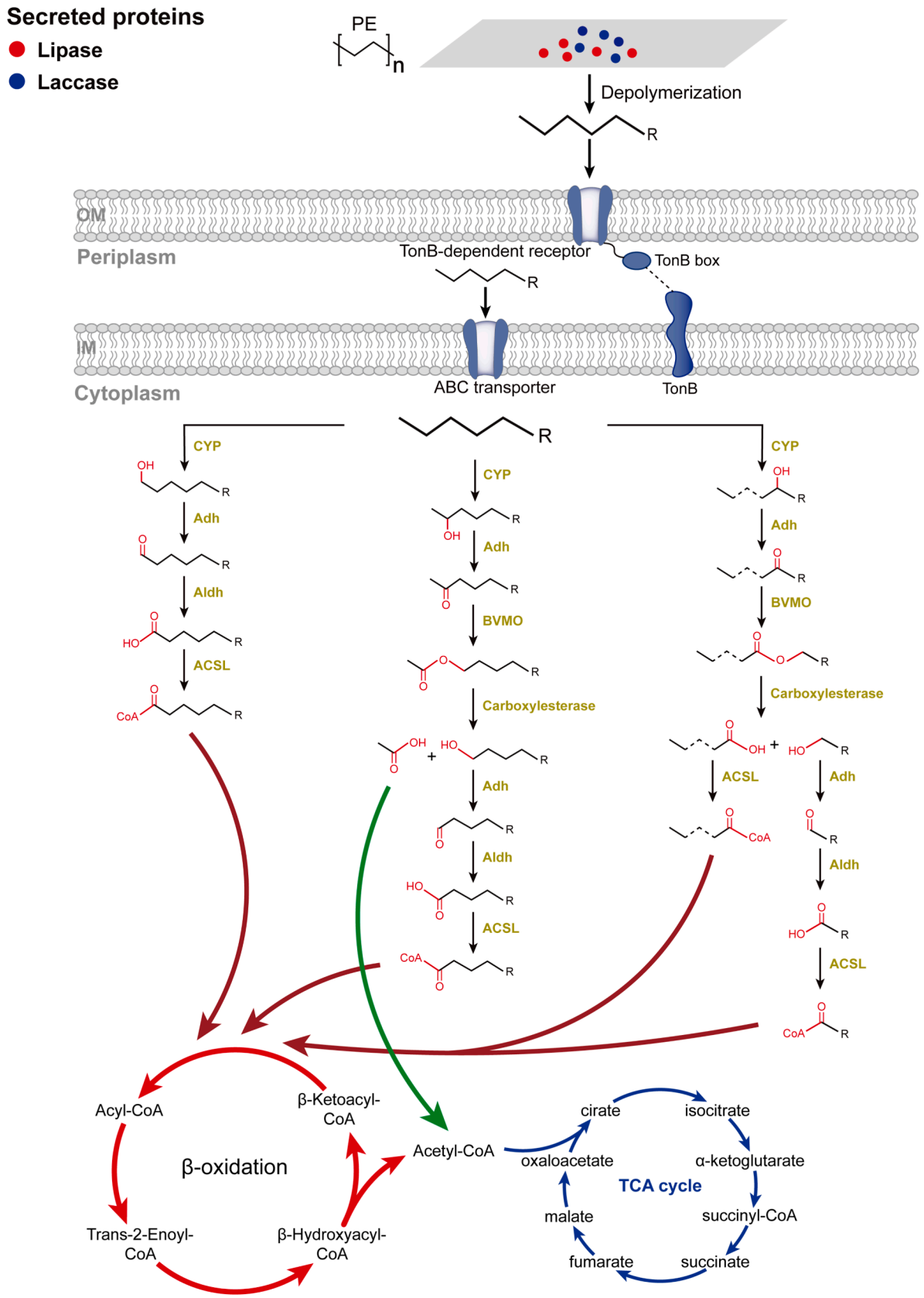

Fig. 6. Putative PE degradation pathway was reconstructed from the enriched microbial community. Abbreviations: CYP, cytochrome P450; Adh, alcohol dehydrogenase; BVMO, Baeyer–Villiger monooxygenase; Aldh, aldehyde dehydrogenase; ACSL, Long-chain fatty acyl-CoA synthetase.

showed the potential to degrade petroleum with the main component of alkanes and thus to remediate the petroleum pollution.

3.5. The proposed PE degradation pathway in the microbial community

Based on the potential PE degradation gene characteristics of the MAGs and previous studies, we propose the PE degradation pathway in the enriched microbial community (Fig. 6). Since multiple MAGs carry potential PE depolymerase genes (Fig. 5), the initial depolymerization of PE may be completed cooperatively by a variety of bacteria in the community, and laccase can be responsible for the initial oxidation of PE. Oxygen was inserted when long PE chains were oxidized, and the oxygen-containing functional group carbonyl was formed and observed in the FTIR results (Fig. 1). Subsequently, the carbonyl groups can be further oxidized to ester, and lipase may be involved in catalyzing the hydrolysis of the ester group on the PE chain, causing the PE chain broken to form short chains or monomers (alkanes).

As mentioned above, MAG4, MAG10, MAG16, MAG18, MAG20, MAG21 and MAG25 all had the potential to fully metabolize alkanes. However, except for the MAG10 as dominated MAG, the abundances of other MAGs were too low or decreased in experimental group compared with the PC group (Fig. 4), so we speculated that MAG10 played a major role in uptaking and metabolism of alkanes. Therefore, the subsequent conceptual model of the alkane degradation pathway was based on MAG10 (Fig. 6). Alkanes enter the periplasm through the TonB system of MAG10 and subsequently enter the cytoplasm through the inner membrane protein ABC transporter. AlkB is also an inner membrane protein, which can serve as a carrier protein to transport alkanes and catalyze alkanes into alcohols (Jeon and Kim, 2016; Rojo, 2009). However, MAG10 not encoded AlkB, so the hydroxylation of alkanes may be conducted by cytochrome P450. Unlike AlkB which can only hydroxylate alkanes with terminal and sub-terminal, cytochrome P450 can hydroxylate the alkanes at different carbon positions (terminal, subterminal and mid-chain) (Yeom et al., 2022). Accordingly, alkanes were subsequently converted into primary and secondary alcohols after hydroxylation by cytochrome P450 in MAG10 (Fig. 6). The primary and secondary alcohols are oxidized into acetate and long-chain fatty acids through a series of cascade enzymatic reactions in intracellular space. The resulting acetate and long-chain fatty acids are respectively synthesized to acetyl-CoA and acyl-CoA and respectively enter the TCA cycle and β-oxidation cycle (Fig. 6). Eventually, metabolites and biodegradation products of PE were assimilated and mineralized into CO_2, H_2O and biomass through the intracellular enzymatic pathway.

4. Conclusions

In summary, a microbial community with PE degradation ability was successfully enriched and screened from AS. The analyses of FTIR, weight loss, contact angle, and HPLC-MS/MS revealed the biodegradation of PE by the enriched community. Several new functional groups, including ether bonds, carbonyl groups, and hydroxyl groups, were detected on the surface of PE via FTIR. Additionally, the weight and hydrophobicity of PE films also decreased after inoculation by the enriched microbial community. HPLC-MS/MS analysis indicated that the addition of PE caused significant changes of the metabolite composition. Lastly, MAGs with PE-degrading potential were retrieved through metagenomic analysis, and a pathway for the AS enriched community to synergistically degrade PE was proposed and to be verified in further study. The results demonstrate that AS from the wastewater treatment plant could serve as a potential microbial source for plastic biodegradation to address the global (micro)plastic crisis in a promising and sustainable way.

CRediT authorship contribution statement

Qihao Li: Writing – review & editing, Writing – original draft, Visualization, Validation, Software, Investigation, Formal analysis, Data curation, Conceptualization. **Huixin Li:** Writing – review & editing, Writing – original draft, Software, Investigation. **Li Tian:** Writing – review & editing, Software, Data curation. **Yicheng Wang:** Writing – review & editing, Software. **Zeping Ouyang:** Writing – review & editing. **Liguan Li:** Writing – review & editing. **Yanping Mao:** Writing – review & editing, Supervision, Project administration, Methodology, Funding acquisition, Conceptualization.

Declaration of competing interest

The authors declare that they have no known competing financial interests or personal relationships that could have appeared to influence the work reported in this paper.

Acknowledgments

This work was funded by Natural Science Foundation of Guangdong Province (2023A1515012019); Shenzhen Science and Technology Program (No. KCXFZ20230731093959008, KCXFZ20240903094205008); The Mentoring Program at Jutu College of Shenzhen University.

Appendix A. Supplementary data

Supplementary data to this article can be found online at https://doi.org/10.1016/j.envint.2025.109334.

Data availability

Data will be made available on request.

References

Alneberg, J., Bjarnason, B.S., De Bruijn, I., Schirmer, M., Quick, J., Ijaz, U.Z., Lahti, L., Loman, N.J., Andersson, A.F., Quince, C., 2014. Binning metagenomic contigs by coverage and composition. Nat. Methods 11 (11), 1144–1146.

Bankevich, A., Nurk, S., Antipov, D., Gurevich, A.A., Dvorkin, M., Kulikov, A.S., Lesin, V. M., Nikolenko, S.I., Pham, S., Prjibelski, A.D., 2012. SPAdes: a new genome assembly algorithm and its applications to single-cell sequencing. J. Comput. Biol. 19 (5), 455–477.

Cantalapiedra, C.P., Hernández-Plaza, A., Letunic, I., Bork, P., Huerta-Cepas, J., 2021. eggNOG-mapper v2: functional annotation, orthology assignments, and domain prediction at the metagenomic scale. Mol. Biol. Evol. 38 (12), 5825–5829.

Chaumeil, P.-A., Mussig, A.J., Hugenholtz, P., Parks, D.H., 2020. GTDB-Tk: a toolkit to classify genomes with the Genome Taxonomy Database. Bioinformatics 36 (6), 1925–1927.

Engler, R.E., 2012. The complex interaction between marine debris and toxic chemicals in the ocean. Environ. Sci. Technol. 46 (22), 12302–12315.

Plastics Europe, 2024. Plastics - the fast facts 2024. Available at https://plasticseurope.org/knowledge-hub/plastics-the-fast-facts-2024/ (accessed 22 September, 2024).

Gao, R., Liu, R., Sun, C., 2022. A marine fungus Alternaria alternata FB1 efficiently degrades polyethylene. J. Hazard. Mater. 431, 128617.

Gao, R., Sun, C., 2021. A marine bacterial community capable of degrading poly (ethylene terephthalate) and polyethylene. J. Hazard. Mater. 416, 125928.

Ghatge, S., Yang, Y., Ahn, J.-H., Hur, H.-G., 2020. Biodegradation of polyethylene: a brief review. Appl. Biol. Chem. 63 (1), 1–14.

Gravouil, K., Ferru-Clément, R., Colas, S., Helye, R., Kadri, L., Bourdeau, L., Moumen, B., Mercier, A., Ferreira, T., 2017. Transcriptomics and lipidomics of the environmental strain Rhodococcus ruber point out consumption pathways and potential metabolic bottlenecks for polyethylene degradation. Environ. Sci. Technol. 51 (9), 5172–5181.

Grandclément, C., Seyssiecq, I., Piram, A., Wong-Wah-Chung, P., Vanot, G., Tiliacos, N., Roche, N., Doumenq, P., 2017. From the conventional biological wastewater treatment to hybrid processes, the evaluation of organic micropollutant removal: a review. Water Res. 111, 297–317.

Gregson, B.H., Metodieva, G., Metodiev, M.V., Golyshin, P.N., McKew, B.A., 2018. Differential protein expression during growth on medium versus long-chain alkanes in the obligate marine hydrocarbon-degrading bacterium *Thalassolituus oleivorans* MIL-1. Front. Microbiol. 9, 3130.

Han, Y.-N., Wei, M., Han, F., Fang, C., Wang, D., Zhong, Y.-J., Guo, C.-L., Shi, X.-Y., Xie, Z.-K., Li, F.-M., 2020. Greater biofilm formation and increased biodegradation of polyethylene film by a microbial consortium of *Arthrobacter sp.* and *Streptomyces sp.* Microorganisms 8 (12), 1979.

Jeon, H.J., Kim, M.N., 2016. Comparison of the functional characterization between alkane monooxygenases for low-molecular-weight polyethylene biodegradation. Int. Biodeterior. Biodegrad. 114, 202–208.

Jin, H., Quan, K., He, Q., Kwok, L.-Y., Ma, T., Li, Y., Zhao, F., You, L., Zhang, H., Sun, Z., 2023. A high-quality genome compendium of the human gut microbiome of Inner Mongolians. Nat. Microbiol. 8 (1), 150–161.
Junaid, M., Siddiqui, J.A., Sadaf, M., Liu, S., Wang, J., 2022. Enrichment and dissemination of bacterial pathogens by microplastics in the aquatic environment. Sci. Total Environ. 830, 154720.
Kang, D.D., Li, F., Kirton, E., Thomas, A., Egan, R., An, H., Wang, Z., 2019. MetaBAT 2: an adaptive binning algorithm for robust and efficient genome reconstruction from metagenome assemblies. PeerJ 7, e7359.
Kim, H.-W., Jo, J.H., Kim, Y.-B., Le, T.-K., Cho, C.-W., Yun, C.-H., Chi, W.S., Yeom, S.-J., 2021. Biodegradation of polystyrene by bacteria from the soil in common environments. J. Hazard. Mater. 416, 126239.
Kumar, A., Lakhawat, S.S., Singh, K., Kumar, V., Verma, K.S., Dwivedi, U.K., Kothari, S., Malik, N., Sharma, P.K., 2024. Metagenomic analysis of soil from landfill site reveals a diverse microbial community involved in plastic degradation. J. Hazard. Mater. 480, 135804.
Li, Q., Tian, L., Cai, X., Wang, Y., Mao, Y., 2022. Plastisphere showing unique microbiome and resistome different from activated sludge. Sci. Total Environ. 851, 158330.
Liu, R., Zhao, S., Zhang, B., Li, G., Fu, X., Yan, P., Shao, Z., 2023. Biodegradation of polystyrene (PS) by marine bacteria in mangrove ecosystem. J. Hazard. Mater. 442, 130056.
Lu, H., Diaz, D.J., Czarnecki, N.J., Zhu, C., Kim, W., Shroff, R., Acosta, D.J., Alexander, B. R., Cole, H.O., Zhang, Y., Lynd, N.A., Ellington, A.D., Alper, H.S., 2022. Machine learning-aided engineering of hydrolases for PET depolymerization. Nature 604 (7907), 662–667.
Mashek, D.G., Li, L.O., Coleman, R.A., 2007. Long-chain acyl-CoA synthetases and fatty acid channeling. Future Lipidol. 2 (4), 465–476.
Mehmood, C.T., Qazi, I.A., Hashmi, I., Bhargava, S., Deepa, S., 2016. Biodegradation of low density polyethylene (LDPE) modified with dye sensitized titania and starch blend using *Stenotrophomonas pavanii*. Int. Biodeterior. Biodegrad. 113, 276–286.
Miri, S., Saini, R., Davoodi, S.M., Pulicharla, R., Brar, S.K., Magdouli, S., 2022. Biodegradation of microplastics: Better late than never. Chemosphere 286, 131670.
Olm, M.R., Brown, C.T., Brooks, B., Banfield, J.F., 2017. dRep: a tool for fast and accurate genomic comparisons that enables improved genome recovery from metagenomes through de-replication. ISME J. 11 (12), 2864–2868.
Parks, D.H., Chuvochina, M., Chaumeil, P.-A., Rinke, C., Mussig, A.J., Hugenholtz, P., 2020. A complete domain-to-species taxonomy for Bacteria and Archaea. Nat. Biotechnol. 38 (9), 1079–1086.
Parks, D.H., Imelfort, M., Skennerton, C.T., Hugenholtz, P., Tyson, G.W., 2015. CheckM: assessing the quality of microbial genomes recovered from isolates, single cells, and metagenomes. Genome Res. 25 (7), 1043–1055.
Patro, R., Duggal, G., Love, M.I., Irizarry, R.A., Kingsford, C., 2017. Salmon provides fast and bias-aware quantification of transcript expression. Nat. Methods 14 (4), 417–419.
Peng, B.-Y., Sun, Y., Xiao, S., Chen, J., Zhou, X., Wu, W.-M., Zhang, Y., 2022. Influence of polymer size on polystyrene biodegradation in mealworms (Tenebrio molitor): responses of depolymerization pattern, gut microbiome, and metabolome to polymers with low to ultrahigh molecular weight. Environ. Sci. Technol. 56 (23), 17310–17320.
Postle, K., Larsen, R.A., 2007. TonB-dependent energy transduction between outer and cytoplasmic membranes. Biometals 20, 453–465.
Price, M.N., Dehal, P.S., Arkin, A.P., 2009. FastTree: computing large minimum evolution trees with profiles instead of a distance matrix. Mol. Biol. Evol. 26 (7), 1641–1650.
Qiu, Q., Li, H., Sun, X., Tian, K., Gu, J., Zhang, F., Zhou, D., Zhang, X., Huo, H., 2024. Integrating genomics, molecular docking, and protein expression to explore new perspectives on polystyrene biodegradation. J. Hazard. Mater. 476, 135031.
Reji, L., Cardarelli, E.L., Boye, K., Bargar, J.R., Francis, C.A., 2022. Diverse ecophysiological adaptations of subsurface Thaumarchaeota in floodplain sediments revealed through genome-resolved metagenomics. ISME J. 16 (4), 1140–1152.
Rojo, F., 2009. Degradation of alkanes by bacteria. Environ. Microbiol. 11 (10), 2477–2490.
Saheb Kashaf, S., Almeida, A., Segre, J.A., Finn, R.D., 2021. Recovering prokaryotic genomes from host-associated, short-read shotgun metagenomic sequencing data. Nat. Protoc. 16 (5), 2520–2541.
Santacruz-Juárez, E., Buendia-Corona, R.E., Ramírez, R.E., Sánchez, C., 2021. Fungal enzymes for the degradation of polyethylene: Molecular docking simulation and biodegradation pathway proposal. J. Hazard. Mater. 411, 125118.
Santo, M., Weitsman, R., Sivan, A., 2013. The role of the copper-binding enzyme–laccase–in the biodegradation of polyethylene by the actinomycete Rhodococcus ruber. Int. Biodeterior. Biodegrad. 84, 204–210.
Shen, Y., Bai, X., Zhou, X., Wang, J., Guo, N., Deng, Y., 2022. Whole-genome analysis of starmerella bacillaris CC-PT4 against MRSA, a non-Saccharomyces yeast isolated from grape. J. Fungi 8 (12), 1255.
Singh, S.P., Sharma, P., Bano, A., Nadda, A.K., Varjani, S., 2022. Microbial communities in plastisphere and free-living microbes for microplastic degradation: A comprehensive review. Green Anal. Chem. 3, 100030.
Sun, Y., Yuan, J., Zhou, T., Zhao, Y., Yu, F., Ma, J., 2020. Laboratory simulation of microplastics weathering and its adsorption behaviors in an aqueous environment: A systematic review. Environ. Pollut. 265, 114864.
Tang, Y., Liu, Y., Chen, Y., Zhang, W., Zhao, J., He, S., Yang, C., Zhang, T., Tang, C., Zhang, C., Yang, Z., 2021. A review: Research progress on microplastic pollutants in aquatic environments. Sci. Total Environ. 766, 142572.
Thompson, R.C., Olsen, Y., Mitchell, R.P., Davis, A., Rowland, S.J., John, A.W.G., McGonigle, D., Russell, A.E., 2004. Lost at sea: Where is all the plastic? Science 304 (5672), 838.
Uritskiy, G.V., DiRuggiero, J., Taylor, J., 2018. MetaWRAP—a flexible pipeline for genome-resolved metagenomic data analysis. Microbiome 6, 1–13.
Wright, R.J., Erni-Cassola, G., Zadjelovic, V., Latva, M., Christie-Oleza, J.A., 2020. Marine plastic debris: a new surface for microbial colonization. Environ. Sci. Technol. 54 (19), 11657–11672.
Wu, H., Liu, Q., Sun, W., Lu, Y., Qi, Y., Zhang, H., 2023. Biodegradability of polyethylene mulch film by *Bacillus paramycoides*. Chemosphere 311, 136978.
Wu, Y.-W., Simmons, B.A., Singer, S.W., 2016. MaxBin 2.0: an automated binning algorithm to recover genomes from multiple metagenomic datasets. Bioinformatics 32 (4), 605–607.
Yan, L., Yang, M., Guo, H., Yang, L., Wu, J., Li, R., Liu, P., Lian, Y., Zheng, X., Yan, J., Huang, J., Li, M., Wu, X., Wen, L., Lao, K., Li, R., Qiao, J., Tang, F., 2013. Single-cell RNA-Seq profiling of human preimplantation embryos and embryonic stem cells. Nat. Struct. Mol. Biol. 20 (9), 1131–1139.
Yang, J., Yang, Y., Wu, W.-M., Zhao, J., Jiang, L., 2014. Evidence of polyethylene biodegradation by bacterial strains from the guts of plastic-eating waxworms. Environ. Sci. Technol. 48 (23), 13776–13784.
Yang, Y., Yang, J., Wu, W.-M., Zhao, J., Song, Y., Gao, L., Yang, R., Jiang, L., 2015. Biodegradation and mineralization of polystyrene by plastic-Eating mealworms: Part 2. Role of gut microorganisms. Environ. Sci. Technol. 49 (20), 12087–12093.
Yao, C., Xia, W., Dou, M., Du, Y., Wu, J., 2022. Oxidative degradation of UV-irradiated polyethylene by laccase-mediator system. J. Hazard. Mater. 440, 129709.
Yeom, S.-J., Le, T.-K., Yun, C.-H., 2022. P450-driven plastic-degrading synthetic bacteria. Trends Biotechnol. 40 (2), 166–179.
Yoshida, S., Hiraga, K., Takehana, T., Taniguchi, I., Yamaji, H., Maeda, Y., Toyohara, K., Miyamoto, K., Kimura, Y., Oda, K., 2016. A bacterium that degrades and assimilates poly (ethylene terephthalate). Science 351 (6278), 1196–1199.
Yu, G., Smith, D.K., Zhu, H., Guan, Y., Lam, T.T.Y., 2017. GGTREE: an R package for visualization and annotation of phylogenetic trees with their covariates and other associated data. Methods Ecol. Evol. 8 (1), 28–36.
Yue, W., Yin, C.-F., Sun, L., Zhang, J., Xu, Y., Zhou, N.-Y., 2021. Biodegradation of bisphenol-A polycarbonate plastic by *Pseudoxanthomonas sp.* strain NyZ600. J. Hazard. Mater. 416, 125775.
Zadjelovic, V., Erni-Cassola, G., Obrador-Viel, T., Lester, D., Eley, Y., Gibson, M.I., Dorador, C., Golyshin, P.N., Black, S., Wellington, E.M., 2022. A mechanistic understanding of polyethylene biodegradation by the marine bacterium Alcanivorax. J. Hazard. Mater. 436, 129278.
Zhang, Y., Pedersen, J.N., Eser, B.E., Guo, Z., 2022a. Biodegradation of polyethylene and polystyrene: From microbial deterioration to enzyme discovery. Biotechnol. Adv., 107991
Zhang, Y., Zhang, T., 2023. Culturing the uncultured microbial majority in activated sludge: a critical review. Crit. Rev. Environ. Sci. Technol. 53 (5), 601–624.
Zhang, Z., Peng, H., Yang, D., Zhang, G., Zhang, J., Ju, F., 2022b. Polyvinyl chloride degradation by a bacterium isolated from the gut of insect larvae. Nat. Commun. 13 (1), 5360.